Food Chemistry 261 (2018) 57–65

Contents lists available at ScienceDirect

Food Chemistry

journal homepage: www.elsevier.com/locate/foodchem

The major glucosinolate hydrolysis product in rocket (*Eruca sativa* L.), sativin, is 1,3-thiazepane-2-thione: Elucidation of structure, bioactivity, and stability compared to other rocket isothiocyanates

Jana Fechner[a,b], Martin Kaufmann[c], Corinna Herz[d], Daniela Eisenschmidt[e], Evelyn Lamy[d], Lothar W. Kroh[c], Franziska S. Hanschen[a,*]

[a] Plant Quality and Food Security, Leibniz Institute of Vegetable and Ornamental Crops, Theodor-Echtermeyer-Weg 1, 14979 Grossbeeren, Germany
[b] Technische Universität Dresden, Chair of Food Chemistry, Bergstrasse 66, 01062 Dresden, Germany
[c] Department of Food Chemistry and Analysis, Institute of Food Technology and Food Chemistry, Technische Universität Berlin, TIB 4/3-1, Gustav-Meyer-Allee 25, 13355 Berlin, Germany
[d] Molecular Preventive Medicine, Institute for Infection Prevention and Hospital Infection Control, Medical Center, University of Freiburg, Breisacher Str. 115b, 79106 Freiburg, Germany
[e] Department of Bioorganic Chemistry, Leibniz Institute of Plant Biochemistry, Weinberg 3, 06120 Halle, Germany

ARTICLE INFO

Keywords:
4-Mercaptobutyl isothiocyanate
1,3-Thiazepane-2-thione
Glucosinolates
Nuclear magnetic resonance (NMR)
Cooking
Reactivity
Cyclization
Rocket

ABSTRACT

Rocket is rich in glucosinolates and valued for its hot and spicy taste. Here we report the structure elucidation, bioactivity, and stability of the mainly formed glucosinolate hydrolysis product, namely sativin, which was formerly thought to be 4-mercaptobutyl isothiocyanate. However, by NMR characterization we revealed that sativin is in fact 1,3-thiazepane-2-thione, a tautomer of 4-mercaptobutyl isothiocyanate with 7-membered ring structure and so far unknown. This finding was further substantiated by conformation sampling using molecular modeling and total enthalpy calculation with density functional theory. During aqueous heat treatment sativin in general was quite stable, while the isothiocyanates erucin and sulforaphane were labile, having half-lives of 132 min and 56 min (pH 5, 100 °C), respectively. Moreover, using a WST-1 assay, we found that sativin did not reduce cell viability of HepG2 cells in a range of 0.3–30 μM, and, therefore, exhibited no cytotoxic effects in this cell line.

1. Introduction

Rocket (*Eruca sativa* L.) is a green leafy Brassicaceae vegetable rich in glucosinolates (GLSs), which are sulfur-containing secondary plant metabolites. GLSs are *NO*-sulfated *β*-D-glucosyl thiohydroximates with a variable (and amino acid-derived) side-chain. Among the more than 130 GLSs identified so far (Agerbirk & Olsen, 2012), rocket contains GLSs of exceptional structure. In detail, the main GLS in *E. sativa* as well as in *Diplotaxis tenuifolia* is 4-mercaptobutyl GLS (4MB; glucosativin) and its oxidized form, the bis(butyl GLS)disulfide (also called dimeric 4 MB), is also present (Bennett et al., 2002; Cataldi, Rubino, Lelario, & Bufo, 2007). Moreover, in *E. sativa*, 4-(*β*-D-glucopyranosyldisulfanyl) butyl GLS (Kim, Jin, & Ishii, 2004) and 4-(cystein-*S*-yl)butyl GSL (Kim et al., 2007) can be found. Next to these "exotic" GLSs, other widely distributed GLSs are present, such as 4-(methylthio)butyl (4MTB; glucoerucin) and 4-(methylsulfinyl)butyl (4MSOB; glucoraphanin) GLS. 4MB is probably formed by demethylation from 4MTB during ontogeny, since *E. sativa* seeds are rich in 4MTB, but leaves and seedlings contain mainly 4MB (Bennett, Rosa, Mellon, & Kroon, 2006). GLSs, such as 4MSOB, are linked with chemopreventive and health-promoting effects and valued especially for their cancer preventive potential (Veeranki, Bhattacharya, Tang, Marshall, & Zhang, 2015). However, these activities are not linked to the GLSs themselves, but rather, to their corresponding isothiocyanates (ITCs), since these GLS hydrolysis products show a range of bioactive functions (Hanschen, Lamy, Schreiner, & Rohn, 2014). Upon cell disruption, GLSs encounter the enzyme myrosinase, which releases glucose and a thiohydroximate-*O*-sulfate. This aglucon can subsequently degrade *via* a Lossen-like rearrangement to the ITC or, especially at low pH, can decompose to the corresponding nitrile. Several genera of the Brassicaceae family also form specific proteins that interact in the degradation of the aglucon, upon which epithionitriles or thiocyanates can also be formed (Burow & Wittstock,

* Corresponding author.
E-mail addresses: fechner_jana@web.de (J. Fechner), martin.kaufmann@tu-berlin.de (M. Kaufmann), corinna.herz@uniklinik-freiburg.de (C. Herz), daniela.eisenschmidt@ipb-halle.de (D. Eisenschmidt), evelyn.lamy@uniklinik-freiburg.de (E. Lamy), lothar.kroh@tu-berlin.de (L.W. Kroh), hanschen@igzev.de (F.S. Hanschen).

https://doi.org/10.1016/j.foodchem.2018.04.023
Received 18 January 2018; Received in revised form 6 April 2018; Accepted 9 April 2018
Available online 10 April 2018

2009). With regard to the volatile GLS hydrolysis products, ITCs have been particularly shown to be reactive substances. Due to their electrophilic C-atom, ITCs readily react with nucleophiles, such as hydroxyl-, amino-, or thiol groups, and then form *O*-thiocarbamates, thiourea derivatives, or dithiocarbamates (Drobnica, Kristián, & Augustín, 1977; Zhang & Talalay, 1994). While reactions with hydroxyl- or amino groups occur only at higher pH, thiols, such as cysteines and glutathione, readily react with ITCs at plant pH values and room temperature (Hanschen et al., 2012; Podhradský, Drobnica, & Kristian, 1979). In aqueous solution, ITCs can also undergo further reactions, e.g., *via* base-catalyzed degradation to the amine, a symmetric thiourea can be formed. Moreover, allyl ITC and 4-(methylsulfinyl)butyl ITC (sulforaphane, 4MSOB-ITC) were shown to release several volatile breakdown products (Chen & Ho, 1998; Jin, Wang, Rosen, & Ho, 1999; Pecháček, Velíšek, & Hrabcová, 1997). Regarding the structure of 4-mercaptobutyl ITC (sativin), which is released from the main GLS in rocket, we expected a high reactivity, as the compound contains a thiol group in addition to the ITC function.

Therefore, this study investigates the reactivity and stability of sativin. Moreover, the structure of sativin was studied applying NMR spectroscopic experiments. Furthermore, its biological activity was investigated *in vitro* in the human liver cancer cell line HepG2 using the WST-1 assay (cell viability assay).

2. Materials and methods

2.1. Chemicals and buffers

Benzonitrile (≥99.9%), KH_2PO_4, Na_2HPO_4, CH_3COOK, methylene chloride-d_2 (≥99.9%), and Triton X-100 (laboratory grade) were purchased from Sigma-Aldrich Chemie GmbH, (Steinheim, Germany). Acetic acid (100%), L-glutathione (GSH; ≥98%), and methylene chloride (GC Ultra Grade) were obtained from Carl Roth GmbH (Karlsruhe, Germany). Ethanol (absolute) and Na_2SO_4 (≥99%) were purchased from VWR International GmbH (Darmstadt, Germany). 4-(Methylthio)butyl ITC (4MTB-ITC, ≥98%) was purchased from Santa Cruz Biotechnology (Heidelberg, Germany) and 4MSOB-ITC was purchased from Enzo Life Sciences GmbH (Lörrach, Germany). Acetonitrile and methanol (LC-MS grade) were purchased from Th. Geyer GmbH & Co. KG (Renningen, Germany). Dulbeccos Minimal Essential Medium (DMEM), fetal calf serum (FCS), L-glutamine (200 mM) and phosphate-buffered saline (without Ca and Mg), penicillin–streptomycin (P/S) solution, trypsin 10× (25 mg/mL), and trypsin-EDTA 10× (5 mg/mL and 2 mg/mL, respectively) were purchased from Life Technologies GmbH (Darmstadt, Germany). Dimethyl sulfoxide (DMSO, ≥99%) was from Applichem (Darmstadt, Germany). All solvents were of LC-MS grade and water was of Milli-Q quality.

2.2. Plant material

Seeds of *Eruca sativa* L. (N.L. Chrestensen Erfurter Samen- und Pflanzenzucht GmbH, Erfurt, Germany) were sown on a wet fleece put on a perlite/water mixture filled in an aluminum tray. Sprouts were grown in a greenhouse for 9 days and watered when needed. Subsequently, sprouts were harvested and mixed with 1.5 parts of water. The mixture was then homogenized using a T25 digital ULTRA-TURRAX® (IKA®-Werke GmbH & Co. KG, Staufen, Germany) and the homogenate was used for the experiments to gauge the stability of ITCs.

2.3. Studies of ITC stability in model systems and in E. sativa plant matrices

To investigate the reactivity of the *E. sativa* ITCs, 500 mg of the plant homogenate as prepared in Section 2.2 were weighed into a 20-mL headspace vial. After which, either 0.5 mL of purified water (treatment at pH 5.2) or 0.5 mL of phosphate buffer (1/15 M, pH 7.6) were added to adjust the pH of the mixtures to pH 7.3. Vials were then closed and samples were left at room temperature (RT) or treated at 100 °C in a block thermoshaker (type MHR 11; Ditabis AG, Pforzheim, Germany) under continuous shaking for 0, 15, 30, and 60 min (come-up time to 95 °C: 3.5 min). After treatment, samples were cooled on ice and subjected to analysis by GC-MS. Each treatment was carried out in triplicate.

For the thermal treatment of purified ITCs (model systems), 2 mL of 1 mM solutions of 4MTB-ITC, 4MSOB-ITC, or purified sativin (see Section 2.5) (0.75 mM) were treated in phosphate buffer (pH 5.0 or pH 7.0, 1/15 M) for 0, 5, 15, 30, 60, and 120 min at 100 °C as described above. Each treatment was carried out in triplicate.

2.4. Analysis of ITC stability by GC–MS

Analysis of 4MTB-ITC and 4MSOB-ITC-stability was performed as reported previously (Hanschen & Schreiner, 2017). Briefly, after treatment, ITCs were extracted using methylene chloride in the presence of 0.2 µmol of the internal standard (IST) benzonitrile. Extracts were dried using anhydrous Na_2SO_4, concentrated under nitrogen gas flow to 300 µL, transferred into a vial, and analyzed by GC-MS using the Agilent 7890A Series GC System (Agilent Technologies) equipped with an Agilent 5975C inert XL MSD and an SGE BPX5 column (30 m × 0.25 mm × 0.25 µm; VWR International GmbH, Darmstadt, Germany), as reported previously (Hanschen & Schreiner, 2017). For measurements on a SolGel1-MS column (30 m × 0.25 mm × 0.25 µm; VWR International GmbH, Darmstadt, Germany) the compounds were separated with a temperature gradient of 9 °C/min after an initial 3 min at 35 °C. For *E. sativa* and model sativin samples, the scan range was between *m/z* 30 and 500. The ITCs were quantified *via* the IST benzonitrile, using their response factors. Each analysis consisted of three independent replicates. ITC degradation was expressed as % to the corresponding untreated control.

2.5. Extraction of sativin for NMR measurement and thermal degradation experiments

For isolation of sativin from *E. sativa*, 65 g *E. sativa* sprouts were mixed 1:1 with water, homogenized as described above, and then methanol was added to a final methanol concentration of 20%. The homogenate was then centrifuged at 2200*g* and 5 °C for 10 min. The supernatant was poured into a flask and methanol was evaporated using a rotary evaporator. Half of the mixture was then added to a 5 g CROMABOND® C18 ec SPE column (Macherey-Nagel GmbH & Co. KG, Düren, Germany) pre-conditioned with 10 mL of ethanol and 20 mL of water. The column was then washed with 10 mL followed by once with 5 mL of water and then several 5-mL volumes of 10% ethanol were used for elution and fractions were collected. After which, 200 µL of each fraction were extracted with methylene chloride, as described above, and analyzed by GC-MS. Sativin was detected in 5-mL fractions 4, 5, and 6 of 10% ethanol, while 4MTB-ITC and 4MSOB-ITC eluted later (4MTB-ITC in fraction 10, 4MSOB-ITC in fractions 8–10).

Sativin-containing fractions were combined. The compounds were then extracted from the combined SPE eluates using methylene chloride; 12 mL of 10% ethanol fractions were diluted with 60 mL of water and then extracted twice with 6 mL and once with 2 mL of methylene chloride. The combined methylene chloride extracts were dried using anhydrous Na_2SO_4 and subsequently under nitrogen. The purified sativin extract (yellowish powder) was stored at −80 °C. For NMR analysis, the extracted sativin was dissolved in methylene chloride-d_2 or in a mixture of DMSO-d_6 and D_2O. An aliquot of this sample was also analyzed by GC-MS to check purity (≥99%). For thermal degradation of purified sativin, a batch of the purified sativin (ca. 15 mg) was dissolved in 200 µL of acetonitrile and diluted with 40 mL of phosphate buffer (1/15 M, pH 5.0 or pH 7.0).

2.6. Structure identification by nuclear magnetic resonance spectroscopy

NMR data were recorded on a Bruker AVANCE III 500 NMR (Bruker Corporation, Rheinstetten, Germany) spectrometer operating at either 500.13 MHz (^{1}H NMR) or 125.76 MHz (^{13}C NMR) and applying standard 1D and 2D NMR experiments (^{1}H, ^{13}C, DEPT, COSY, HSQC, HMBC). NMR chemical shifts were referenced to internal tetramethylsilane (TMS). Chemical shifts as well as coupling constants of sativin were determined by iterative spectra simulations using the TopSpin implement Daisy (Bruker BioSpin GmbH, Rheinstetten).

2.7. Characterization of the UV–Vis spectrum of sativin and 4MTB-ITC and identification of glutathione-adducts using UHPLC-DAD-TOF

For the UV spectrum measurement, 1 mL of methanol was added to 300 mg of homogenized fresh *E. sativa* sprouts, followed by shaking (30 s) and centrifugation at 2150*g* for 5 min. For GSH-adducts identification of ITC, sprouts were either homogenized in the presence of 0.5 mM GSH or water; after 30 min the homogenate was mixed with ethanol (1:1) and centrifuged as described above. The supernatant was then centrifuged through an Amicon Ultra 0.5 mL centrifugal filter MWCO 3 kDa (Sigma-Aldrich Chemie GmbH). 4MTB-ITC was dissolved in acetonitrile. After injection of 2 µL of sample into an Agilent UHPLC-DAD-TOF system [Agilent Technologies Deutschland GmbH & Co. KG, Waldbronn, Germany; binary pump (G7120A), diode array detector (DAD, G7117A), oven (G7116B), autosampler (G7167B), MS-TOF (G6230B)] equipped with a Poroshell 120 EC-C18, 2.1 × 100 mm, 2.7 µm, analytes were separated with a flow of 0.4 mL/min at 30 °C using a gradient of water (**A**) and acetonitrile (**B**), starting from 2% **A** and increasing to 100% **B** within 20 min (2 min hold) and then returning within 1 min to the initial settings (5 min equilibration time). The DAD range was 200–400 nm. MS-TOF parameters were as follows: positive ionization, mixed ion mode, gas temperature 325 °C, vaporizer 200 V, gas flow 8 L/min, VCharge 2000 V, nebulizer 35 psig, VCap 2500 V, skimmer1 65 V, fragmentor 175 V, corona positive 4 V, octopole RF peak 750 V, mass range *m/z* 90–1000 .

2.8. Fitting of data

Results from the degradation of the compounds during aqueous thermal treatment in model systems and in a plant matrix could be fitted by a first order kinetic model with $[A]_t$ being the concentration at a certain time (t), $[A]_0$ being the concentration at the beginning (t = 0 min), k being the reaction rate constant (min^{-1}), and $t_{1/2}$ being the half-life period [min] (time when 50% are degraded):

$$[A]_t = [A]_0 \cdot e^{-k \cdot t}$$

$$t_{1/2} = \ln 2/k$$

2.9. Molecular modeling

The systematical conformational search around all single bonds of 4-mercaptobutyl-ITC was performed in MOE2016.08 (Molecular Operating Environment, Chemical Computing Group Inc., Montreal, QC, Canada). Two conformations are deemed equal if the root mean square deviation of the superposition was less than 0.25 Å. In a first step, all structures were geometry optimized and energy minimized using the Amber10:EHT force field and the Generalized Born implicit water model. For a more precise energy calculation, a DFT approach in ORCA 3.0 using the functional B3LYP (Becke, 1992; Lee, Yang, & Parr, 1988; Stephens, Devlin, Chabalowski, & Frisch, 1994; Vosko, Wilk, & Nusair, 1980) with the def2-SVP (Weigend, 2006) basis set was used. All calculations were done in water using the Conductor-like Screening Model (COSMO) (Klamt & Schuurmann, 1993). To deduce the total enthalpy of the considered molecules, numerical frequencies were calculated (keyword NumFreq). Dispersion corrections were calculated with the Becke-Johnson damping function (D3BJ) and enabled a more detailed description of long-range interactions between unbound atoms (Becke & Johnson, 2005). The tautomeric equilibrium and the required activation energy for a proton transfer between 4,5,6,7-tetrahydro-1,3-thiazepine-2-thiol and 1,3-thiazepane-2-thione were investigated by scan calculations and subsequent energy minimization in ORCA 3.0. The equilibrium constant K was calculated with the given equation at T = 298.15 K.

$$K = e^{(-\Delta H/RT)}$$

2.10. Determination of mitochondrial dehydrogenase activity as a parameter for cell viability

The WST-1 assay (Roche Diagnostics Deutschland GmbH, Mannheim, Germany) was used to assess cell viability with liver cancer cell line HepG2 (from the German Collection of Microorganisms and Cell Cultures, Braunschweig, Germany). Cells were cultured in DMEM supplemented with 15% FCS and 1% P/S in a 5% CO_2 atmosphere at 37 °C. The WST-1 assay was carried out as described previously following the manufacturer's instructions (Kupke et al., 2016). Absorbance was measured at 435 nm using a microplate reader (Infinite M200; Tecan, Männedorf, Switzerland). The determination of mitochondrial dehydrogenase activity was performed using four replicates in four independent experiments.

2.11. Statistical analysis

To investigate differences between concentrations at RT (Fig. 1) or half-lives at 100 °C (Fig. 2, Table 1) ANOVA and Tukey's HSD test were performed to compare means at the $p \leq 0.05$ level. A *t*-test was applied to investigate the effect of the pH-value on half-lives at 100 °C of each model compound (Fig. 2, Table 1). STATISTICA version 12 software [StatSoft, Inc. (2013)] was used. Each treatment was carried out in triplicate.

3. Results and discussion

3.1. Stability of rocket ITCs and sativin

In a first approach, the stability of ITCs from rocket sprouts was investigated at room temperature for 24 h. Four compounds were identified by their mass spectra in the rocket sprout homogenate: 4MTB-ITC (erucin) from 4MTB, 4MSOB-ITC from 4MSOB, and bis(4-isothiocyanatobutyl)disulfide (bisITCButDS) (Bennett et al., 2002; Cerny, Taube, & Battaglia, 1996), as well as sativin from 4MB (Bennett et al., 2002; Cerny et al., 1996). The mass spectrum of sativin is provided in Supplemental Fig. 1 and had a high similarity to that reported by Raffo et al. (2018). The retention index (RI) of sativin determined on the BPX5 column was 1418 and on a SolGel1-MS column (similar to DB-1) was 1297 and thus very similar to that reported previously (Raffo et al., 2018). In total, the rocket sprouts contained 2.27 µmol/g FW GLS hydrolysis products, of which 69% were sativin, 12% were 4MTB-ITC, 12% were 4MSOB-ITC, and 6% were bisITCButDS. This profile and the levels correspond well to that reported by Bennett and co-workers for GLS in *E. sativa* sprouts (Bennett, Carvalho, Mellon, Eagles, & Rosa, 2007). The dimeric bisITCButDS probably derived either from the dimeric 4 MB or by oxidation of sativin. Of note is that bisITCButDS was shown to be formed upon oxidation of sativin with H_2O_2 and its structure was elucidated by NMR (Cerny et al., 1996).

When investigating the stability of the rocket GLS hydrolysis products at room temperature at plant pH (pH 5.2), 4MTB-ITC was least stable at RT and decreased by 74% within 5 h (Fig. 1A). 4MSOB-ITC was more stable and decreased only by 31% within 24 h. Surprisingly, sativin showed no decrease, but 40% higher concentrations were

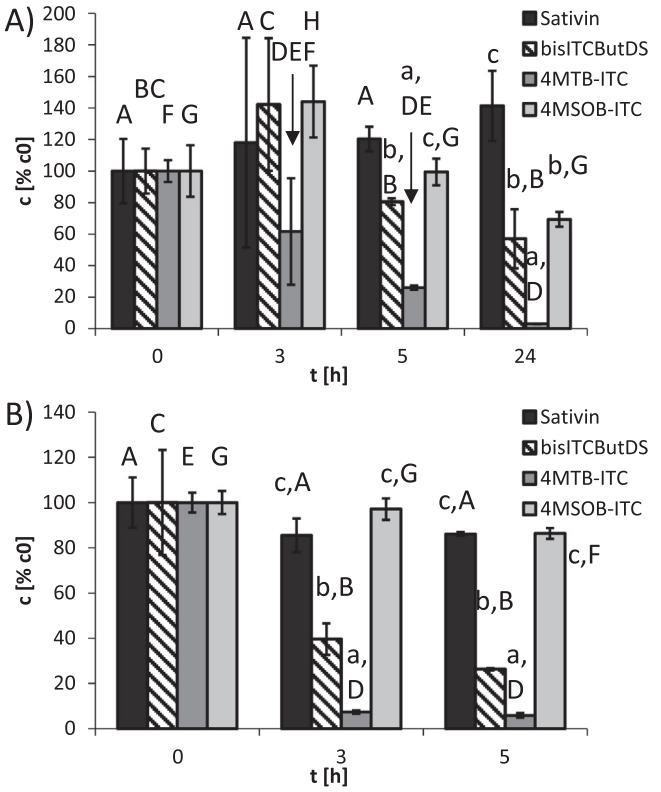

Fig. 1. Stability of Isothiocyanates (ITCs) and derivatives in an *E. sativa* matrix at room temperature at A) plant pH (pH 5.2) and B) pH 7.4 over time. Lower case letters indicate significant differences between relative concentrations of different compounds at one treatment time. Capital letters indicate significant differences between treatment times for one compound. Fig. 1A: Sativin (A), bisITCButDS (B and C), 4MTB-ITC (D–F), 4MSOB-ITC (G and H); Fig. 1B: Sativin (A), bisITCButDS (B and C), 4MTB-ITC (D and E), 4MSOB-ITC (F and G) as tested by ANOVA and Tukey's HSD test at the $p \leq 0.05$ level [$n = 3$, except for 3 h, Fig. 1A $n = 2$)] using STATISTICA version 12 software [StatSoft, Inc. (2013)]. Abbreviations: 4MTB-ITC: 4-methylthiobutyl ITC. 4MSOB-ITC: 4-methylsulfinylbutyl ITC. bisITCButDC: bis(4-isothiocyanatobutyl)disulfide.

detected after 24 h, while concentrations of the dimeric bisITCButDS by tendency decreased by 43% within 24 h (Fig. 1A). At neutral pH conditions after 5 h at RT, 94% of 4MTB-ITC and 74% of bisITCButDS were degraded, while sativin remained stable and 4MSOB-ITC levels decreased by only 14% (Fig. 1B).

We initially postulated that sativin would be more reactive compared to the other ITCs (dimerization etc.). Therefore, to enhance reactivity, *E. sativa* homogenates were treated at 100 °C. At plant pH conditions (pH 5.2) and within 1 h of thermal treatment, no significant decrease was observed for sativin, while the dimeric bisITCButDS and 4MSOB-ITC decreased by 83% and 31%, respectively. Surprisingly, 4MTB-ITC levels increased by 88% (Fig. 2A). ITCs have been reported to readily react with thiols, such as GSH, to form dithiocarbamates at pH 5 (Hanschen et al., 2014). Such ITC-GSH-adducts were also present in homogenized fresh rocket sprouts samples, as tentatively identified via their exact mass (4MTB-ITC-GSH adduct: $[M+H]^+_{calculated} = 469.12437$, $[M+H]^+_{measured} = 469.12388$, $\Delta = 1$ ppm; 4MSOB-ITC-GSH adduct $[M+H]^+_{calculated} = 485.11929$, $[M+H]^+_{measured} = 485.11916$, $\Delta = 1$ ppm). An adduct for sativin was not identified here. However, the resulting dithiocarbamates are not thermally stable and ITCs can again be released (Bruggeman, Temmink, & van Bladeren, 1986; Hanschen et al., 2012). Thus, these "masking effects" might explain elevated 4MTB-ITC concentrations. However, in such a case, it would be expected that other ITCs would increase as well. It is also of note that the stability of 4MSOB-ITC in the plant matrix was also higher compared to a model system at pH 5 (Table 1).

In neutral solution (pH 7.3), in our study, all ITCs were more labile, compared to plant pH conditions (pH 5.2). In the plant matrix after 1 h, 4MTB-ITC and sativin were most stable, decreasing by 84% and 87%, respectively, while bisITCButDS and 4MSOB-ITC were decreased by 97% and 99%, respectively (Fig. 2B).

Subsequently, the stability of isolated sativin was investigated and compared to the synthetic 4MTB-ITC and 4MSOB-ITC in buffered model systems. Compared to the ITCs present in the plant matrix (Fig. 2A and B), the ITCs 4MTB- and 4MSOB-ITC in the model system were more labile at pH 5 (Fig. 2C). Wu and colleagues also reported that 4MSOB-ITC was more labile in a model system than in a broccoli extract in a pH range of between pH 3 and pH 6 (Wu, Mao, You, & Liu, 2014). This finding once again could support the theory of "masked" ITCs in the plant matrix, which are released during thermal treatment under acidic conditions. Under neutral conditions (pH 7), ITCs were more stable in the model (Fig. 2D) compared to ITCs in the plant matrix (pH 7.3). This can also be seen from the half-life data presented in Table 1. The enhanced reactivity of ITCs in the plant matrix might be attributed to the slightly higher pH (pH 7.3) compared to the model (pH 7.0). With regard to the stability of the ITCs, 4MSOB-ITC was the least stable in our study, but a significant difference to 4MTB-ITC was only found using a *t*-test. At pH 5, the half-life of 4MSOB-ITC was just 56 min at 100 °C (Table 1). This finding is in line with a similar study of Wu et al., who observed a half-life for 4MSOB-ITC of 1.12 h at 90 °C [calculated from the given value for k (h^{-1})] (Wu, Mao, Mei, & Liu, 2013).

Surprisingly, in the model, we found that sativin, which was stable compared to the two other ITCs studied, was more labile at pH 5 compared to pH 7 (*t*-test of half-lives: $p = 0.0509$) (Fig. 2C and D, Table 1). In contrast, 4MTB-ITC and 4MSOB-ITC were more stable at pH 5 and their reactivity increased with an increase in pH – a finding that is in line with the literature for ITCs. For example, the increased reactivity of ITCs under basic conditions is due to the facilitated reaction with the hydroxyl ion, which results in the formation of the amine, and finally, in the formation of a symmetrical N,N′-diRthiourea (Chen, Rosen Robert, & Ho, 1998; Drobnica, Kristián, & Augustín, 1977). Therefore, the high stability of sativin and its different behavior compared to the other ITCs studied pointed to a different structure. This hypothesis is further supported by the UV spectra obtained by UHPLC-DAD-TOF (the TOF was used for identification of sativin in the rocket matrix) and presented in Supplemental Fig. 2. In contrast to 4MTB-ITC (Supplemental Fig. 2A) and other ITCs, sativin (Supplemental Fig. 2B) had no maximum at 240 nm, but rather a very different spectrum with a maximum at 286 nm. Such a spectra is similar to that of dithiocarbamates (Budnowski et al., 2013).

3.2. Nuclear magnetic resonance spectroscopy of sativin

Therefore, to clarify the structure of sativin, we isolated the compound and applied NMR spectroscopy. To elucidate the structure of the compound having an *m/z* of 147.0176 ($[M+H]^+$ measured by LC-QTOF: 148.0248, $\Delta m/z = 4.5$ ppm), and therefore, the chemical formula of $C_5H_9NS_2$, standard 1D and 2D NMR experiments (^1H, ^{13}C, DEPT, COSY, HSQC, HMBC) were performed on a Bruker AVANCE III 500 NMR spectrometer operating at 500.13 MHz. Since the compound was dissolved in a mixture of DMSO-d_6 and D_2O, protons bound to hetero-atoms would not be observable due to fast H/D-exchange. The ^1H NMR spectrum of the compound shows four higher order signals with an integral ratio of 1:1:1:1 (Fig. 3; Supplemental Fig. 3 shows the 1H NMR spectrum in methylene chloride). Hence, the molecule is unbranched and consists of four methylene units. In addition, the higher order signals exclude a linear structure. Nevertheless, the COSY spectrum shows that the methylene units are connected to each other, forming an *n*-butylene moiety. According to the chemical formula, the ^{13}C NMR spectrum shows an additional carbon signal resonating at 201.4 ppm. Since the molecule must not be symmetrical due to the existence of four non-equivalent methylene units, this resonance can be

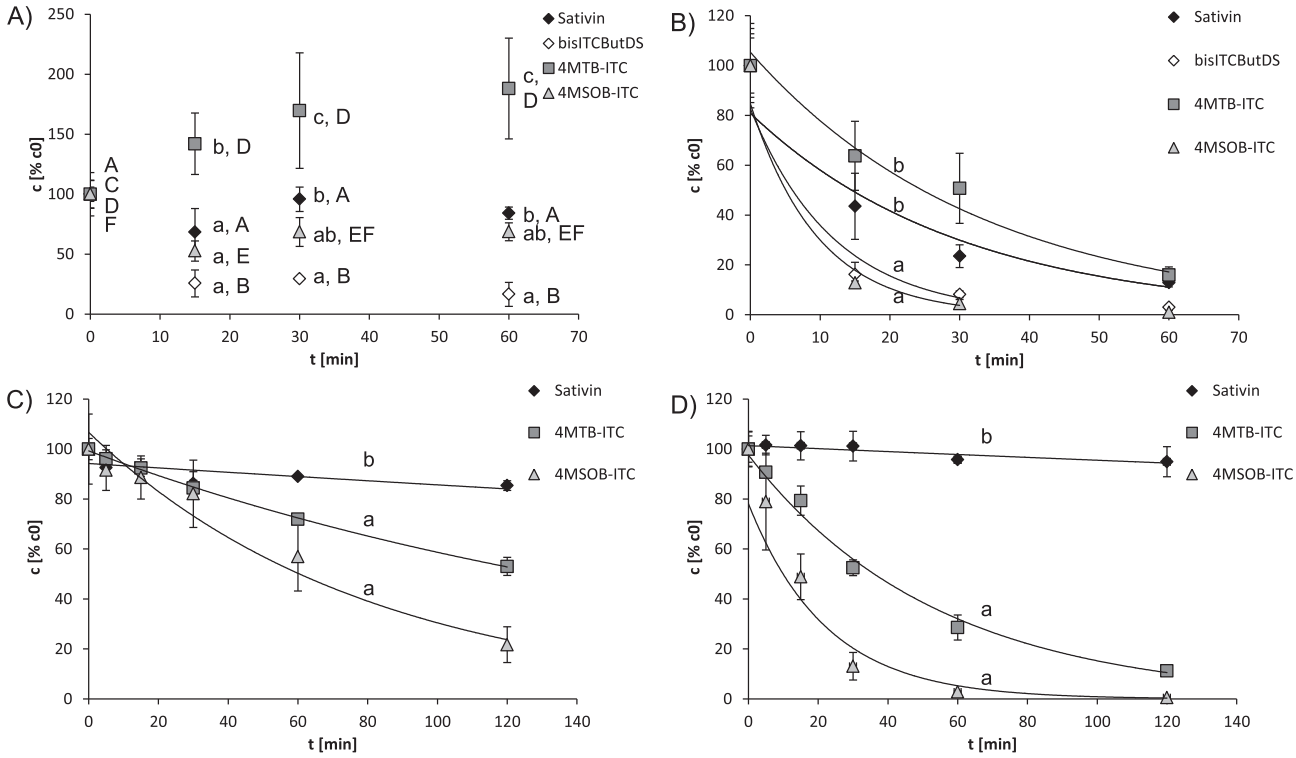

Fig. 2. Stability of isothiocyanates (ITCs) and derivatives thereof during thermal treatment (100 °C) in A) *E. sativa* homogenate at plant pH (pH 5.2), B) *E. sativa* homogenate at pH 7.3, C) isolated or standard compounds at pH 5.0 in model solutions, and D) isolated or standard compounds at pH 7.0 in model solutions. For kinetics of 4MSOB-ITC and bisITCButDS the values of the 60 min treatment were not used for the calculation of the curve as they did not follow a first order degradation any more. Small letters indicate significant differences between relative concentrations (Fig. 2A) or degradation kinetics (half-lives tested) (Fig. 2B–D) as tested by ANOVA and Tukey's HSD test at the $p \leq 0.05$ level ($n = 3$) using STATISTICA version 12 software [StatSoft, Inc. (2013)]. Capital letters in Fig. 2A indicate significant differences between treatment times for one compound: sativin (A), bisITCButDS (B and C), 4MTB-ITC (D), 4MSOB-ITC (E and F). Abbreviations: 4MTB-ITC: 4-methylthiobutyl ITC; 4MSOB-ITC: 4-methylsulfinylbutyl ITC; bisITCButDS: bis(4-isothiocyanatobutyl)disulfide.

assigned to the sp^2 carbon of a dithiocarbamate, which is widely in accordance with the literature (Halimehjani, Marjani, & Ashouri, 2010). The HMBC spectrum shows correlations of the sp^2 carbon to both of the ends of the butylene moiety, thereby suggesting that the respective methylene groups must both be connected to a hetero-atom which is indicated by their chemical shifts. Consequently, the observed HMBC correlations are evoked by $^3J_{C,H}$ couplings. The connection of the assigned structural features results in a seven-membered cyclic dithiocarbamate. The presence of a dithiocarbamate group was also indicated by the UV-spectrum (Supplemental Fig. 2A).

Consequently, sativin was identified as 1,3-thiazepane-2-thione, which can be regarded as the cyclic tautomer of 4-mercaptobutyl ITC. To verify whether there was a solvent-dependent equilibrium between the two possible tautomers, another set of NMR experiments was acquired using deuterated methylene chloride as solvent. However, the acyclic tautomer was neither detectable in aqueous solution nor in the organic solvent. Fig. 4 presents the formation of sativin/1,3-thiazepane-2-thione from 4MB and the formation of their oxidized dimers.

Table 1
Kinetic parameters of isothiocyanate (ITC) and sativin/1,3-thiazepane-2-thione degradation during aqueous thermal heat treatment at 100 °C under different conditions. Abbreviations: 4MSOB-ITC: 4-(methylsulfinyl)butyl ITC; 4MTB-ITC: 4-(methylthio)butyl ITC.

	System	k (min^{-1})	$t_{1/2}$ (min)		R^2
4MSOB-ITC	pH 5.2, plant	0.0063 ± 0.0021	119.65 ± 46.86	B	0.6574 ± 0.2345
4MSOB-ITC	pH 7.3, plant	0.1051 ± 0.0084	6.62 ± 0.53	a, A	0.9657 ± 0.0288
4MTB-ITC	pH 5.2, plant	Increased			
4MTB-ITC	pH 7.3, plant	0.0303 ± 0.0013	22.88 ± 0.94	c	0.9716 ± 0.0232
Sativin	pH 5.2, plant	No degradation			
Sativin	pH 7.3, plant	0.0330 ± 0.0010	21.01 ± 0.61	b	0.9250 ± 0.0452
4MSOB-ITC	pH 5.0, model	0.0128 ± 0.0026	55.92 ± 12.90	a, B	0.9549 ± 0.0321
4MSOB-ITC	pH 7.0, model	0.0450 ± 0.0033	15.45 ± 1.11	c, A	0.9556 ± 0.0215
4MTB-ITC	pH 5.0, model	0.0053 ± 0.0005	132.4 ± 13.1	a, D	0.9924 ± 0.0016
4MTB-ITC	pH 7.0, model	0.0186 ± 0.0009	37.25 ± 1.66	c, C	0.9895 ± 0.0058
Sativin	pH 5.0, model	0.00095 ± 0.00015	743.7 ± 112.8	b, E*	0.5186 ± 0.1248
Sativin	pH 7.0, model	0.00066 ± 0.00010	1061.4 ± 164.5	d, F*	0.6408 ± 0.2232

ANOVA and Tukey's HSD test were performed to compare means of the half-lives at the $p \leq 0.05$ level between compounds treated at pH-value in plant tissue (only pH 7.3 investigated) or in the model. Lower case letters indicate differences between compounds at pH 7.3 in the plant (a–c), or in the model pH 5 (a and b) or pH 7 (c and d). To investigate the effect of the pH-value on half-lives in the plant or in the model, means of half-life at each pH were compared for each compound using *t*-test. Capital letters indicate differences between compounds treated at pH 5 and 7 (4MSOB-ITC: A,B; 4MTB-ITC; Sativin C,D). STATISTICA version 12 software [StatSoft, Inc. (2013)] was used. *$p = 0.0509$.

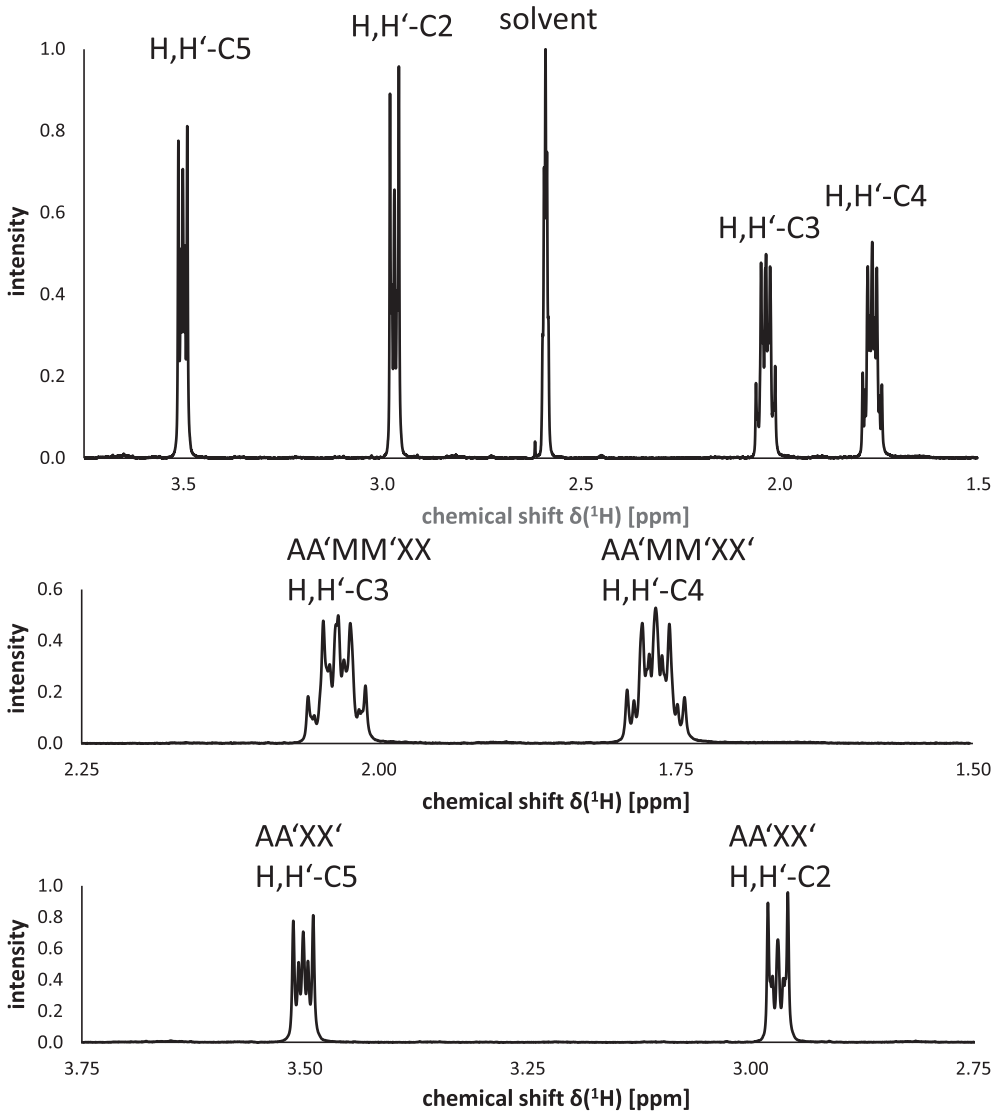

Fig. 3. ^{1}H NMR spectrum of sativin/1,3-thiazepane-2-thione dissolved in a mixture of DMSO-d_6 and D_2O acquired at 500.13 MHz. Spectra were acquired at 296 K and referenced to internal tetramethylsilane (TMS).

Due to the asymmetric structure of the analyzed compound, the methylene protons are magnetically non-equivalent. Thus, the ^{1}H NMR spectrum shows the signals of two AA'XX' as well as two AA'MM'XX' spin systems (Fig. 3). Since the analytical elucidation of such higher order spectra is somewhat cumbersome, ^{1}H chemical shifts and coupling constants were determined by iterative spectral simulations using the TopSpin implement Daisy (Bruker BioSpin GmbH, Rheinstetten). The respective spectral parameters are summarized in Table 2.

3.3. Molecular modeling and DFT approach

To further substantiate the NMR results and to investigate whether the 4-mercaptobutyl ITC, which will be released spontaneously from the GLS aglucon, forms 1,3-thiazepane-2-thione, their thermodynamic equilibrium was calculated, utilizing a molecular modeling and DFT approach. First, a set of different 4-mercaptobutyl ITC conformations was systematically generated in MOE2016.08 [Molecular Operating Environment (MOE), 2016.08; Chemical Computing Group Inc., Montreal, QC, Canada]. This conformation search resulted in 48 different structures with an optimal heavy atom RMS superposition distance of > 0.25 Å. A more stretched side-chain of 4-mercaptobutyl ITC was a feature of the lowest energy conformation. Together with the 1,3-thiazepane-2-thione, the geometries of both structures were further optimized and their enthalpies were calculated. This was performed in implicit water (COSMO) at RT using a DFT approach in ORCA 3.0 (Neese, 2012). The obtained total enthalpies for 4-mercaptobutyl ITC and 1,3-thiazepane-2-thione were $-2747021.28\ kJ\ mol^{-1}$ and $-2747052.00\ kJ\ mol^{-1}$, respectively. After comparing these enthalpies, 1,3-thiazepane-2-thione was found to be $-30.72\ kJ\ mol^{-1}$ more stable than the corresponding 4-mercaptobutyl ITC. This finding indicates that the thermodynamic equilibrium is shifted rightwards to the cyclic tautomer. Furthermore, 1,3-thiazepane-2-thione can rearrange to the related thiol form, (4,5,6,7)-tetrahydro-1,3-thiazepine-2-thiol. Such a thione/thiol tautomerism has been investigated in the literature in detail (Abbehausen, de Paiva, Formiga, & Corbi, 2012; Özdemir & Türkpençe, 2013). To elucidate the predominance of one certain tautomer the total enthalpy of (4,5,6,7)-tetrahydro-1,3-thiazepine-2-thiol was also calculated using DFT. Compared to 1,3-thiazepane-2-thione the corresponding thiol was 114.19 kJ mol^{-1} less stable ($-2746937.81\ kJ\ mol^{-1}$) and emphasized the thione as the thermodynamically most stable structure. A simulation of an intramolecular and intermolecular proton transfer and the required activation energies to rearrange the thiol to the thione is described in the Supplementary Fig. 4. The equilibrium constant K was calculated to get an impression

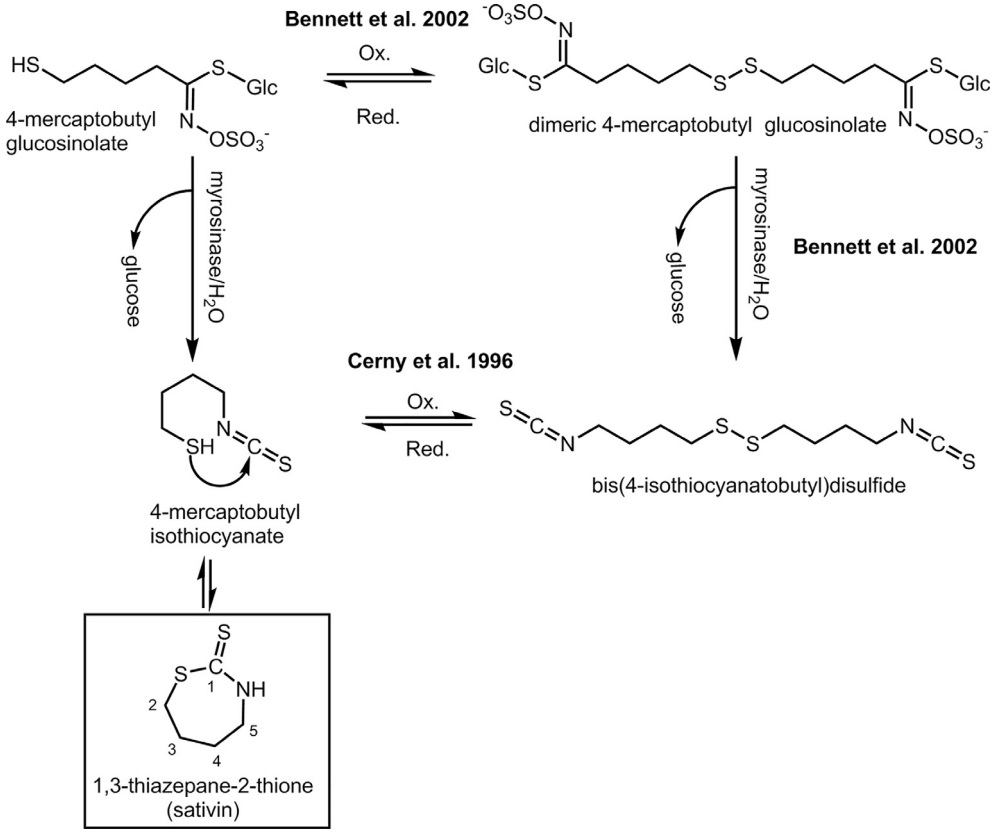

Fig. 4. Enzymatic degradation of 4-mercaptobutyl glucosinolate, its dimerization, and the formation of sativin/1,3-thiazepane-2-thione. Based on the present work and on previous publications (Bennett et al., 2002; Cerny et al., 1996).

of the ratio of both tautomeric structures. Using the total enthalpy difference $K = 9.88 \times 10^{-21}$ indicated that the tautomeric equilibrium is unambiguously shifted to 1,3-thiazepane-2-thione and the corresponding thiol tautomer is not present in solution. These calculations support the notion that sativin from rocket is mainly present as the 1,3-thiazepane-2-thione tautomer.

Cyclization of ITCs from Brassicaceae plants is also known for 2-hydroxyalkenyl ITC. For example, from the GSL progoitrin, the goitrogenic 5-vinyl-1,3-oxazolidine-2-thione is formed, which inhibits the production of thyroid hormones, and, therefore, can be a problem, especially in animal nutrition (Astwood, Greer, & Ettlinger, 1949; Gaitan, 2004). Of note is that 1,3-oxazolidine-2-thiones can isomerize at high temperatures to 1,3-thiazolidine-2-ones, as was observed when injected in a GC-MS system, which can complicate their analysis (Agerbirk & Olsen, 2015; Radulović, Todorovska, Zlatković, Stojanović, & Randjelović, 2017).

3.4. Effects of sativin on cell viability of Hep-G2 cells

To access first data on the bioactivity of sativin, the human liver cancer cell line HepG2 was exposed to different concentrations of sativin (0.3–30 μM) for 72 h and the effect on cell viability was investigated. For this purpose, loss of mitochondrial dehydrogenase activity was analyzed. As shown in Supplemental Fig. 5, no loss of cell viability was detected for any of the concentrations. In contrast to sativin, 4MTB-ITC was shown to inhibit the proliferation and viability of Hep-G2 cells at concentrations higher than 10 μM, as well as to induce apoptosis and cell cycle arrest (Lamy & Mersch-Sundermann, 2009). Thus, cyclization to 1,3-thiazepane-2-thione probably reduces the cytotoxic potential of rocket; therefore the chemopreventive potential, with respect to apoptosis induction or cell cycle arrest, could also be lower compared to ITC. However, as only one cell line was tested, the results might be different with other cell lines. Moreover, 1,3-thiazepane-2-thione might have other health-preventive effects. For example it might increase phase-II metabolism enzymes or have anti-inflammatory effects. Recently, Radulović et al. showed that 1,3-oxazolidine-2-thiones have immunomodulatory effects and can exert nitric oxide production-inhibiting properties (Radulović et al., 2017). Therefore, future studies should investigate 1,3-thiazepane-2-thione to evaluate if this interesting compound contributes to health-preventive effects of Brassicaceae consumption.

3.5. Perspectives

In nature GLSs often occur in homologues and especially methionine-derived GLSs such as 4MB show a great variety. This reflects in the high diversity of hydrolysis products and thus a high diversity of beneficial and toxic effects on health (Agerbirk & Olsen, 2012; Hanschen et al., 2014). This variability in GLS biosynthesis enables plants to respond to their environment. Variation in side-chain structure causes differences in ITC lipophilicity and volatility as well as their reactivity (Agerbirk & Olsen, 2012). For example cyclic products such as the newly identified 1,3-thiazepane-2-thione are usually the result of a nucleophilic function in the side chain, such as a hydroxyl function in 2-position of the side chain, which results in reactive ITC that undergo ring closure and form the goitrogenic oxazolidine-2-thiones. The cyclization to a 7-membered ring product as reported here, to our knowledge has not been observed before in GLS chemistry. So far to our knowledge, homologs of 4MB have not been reported. If one day a 3-mercaptopropyl GLS is found, its ITC probably will also cyclize forming a 6-membered ring. The cyclization of higher homologs of 4-mercaptobutyl ITC, however, will be less favored, due to the higher ring strain of 8-membered rings.

With regard to the flavor of rocket, so far it is believed that 4-

Table 2
^{1}H and ^{13}C chemical shifts [ppm] and homonuclear proton-proton coupling constants [Hz] of sativin (1,3-thiazepane-2-thione) in a mixture of DMSO-d_6 and D_2O as determined by iterative spectral simulations. ^{1}H chemical shifts are given with four decimals to allow the discrimination between magnetically non-equivalent methylene protons. Spectra were acquired at 296 K and referenced to internal tetramethylsilane (TMS). Iterative spectral simulations were carried out using the TopSpin implement Daisy (Bruker BioSpin GmbH, Rheinstetten).

Carbon	δ ^{13}C [ppm]	Proton	δ ^{1}H [ppm]	Coupling constant [Hz]
C–1	201.4	–	–	–
C–2	35.3	*H–C–2*	2.9692	$^{2}J_{2,2'} = -13.6$ $^{3}J_{2,3} = 10.0$ $^{3}J_{2,3'} = 2.2$
		H′–C–2	2.9688	$^{2}J_{2',2} = -13.6$ $^{3}J_{2',3} = 2.1$ $^{3}J_{2',3'} = 8.0$
C–3	27.8	*H–C–3*	2.0352	$^{3}J_{3,2} = 10.0$ $^{3}J_{3,2'} = 2.1$ $^{2}J_{3,3'} = -12.6$ $^{3}J_{3,4} = 6.5$ $^{3}J_{3,4'} = 6.7$
		H′–C–3	2.0350	$^{3}J_{3',2} = 2.2$ $^{3}J_{3',2'} = 8.0$ $^{2}J_{3',3} = -12.6$ $^{3}J_{3',4} = 6.3$ $^{3}J_{3',4'} = 6.5$
C–4	27.6	*H–C–4*	1.7668	$^{3}J_{4,3} = 6.5$ $^{3}J_{4,3'} = 6.3$ $^{2}J_{4,4'} = -12.6$ $^{3}J_{4,5} = 2.7$ $^{3}J_{4,5'} = 8.4$
		H′–C–4	1.7676	$^{3}J_{4',3} = 6.7$ $^{3}J_{4',3'} = 6.5$ $^{2}J_{4',4} = -12.6$ $^{3}J_{4',5} = 8.1$ $^{3}J_{4',5'} = 3.2$
C–5	47.4	*H–C–5*	3.5003	$^{3}J_{5,4} = 2.7$ $^{3}J_{5,4'} = 8.1$ $^{2}J_{5,5'} = -12.5$
		H′–C–5	3.5028	$^{3}J_{5',4} = 8.4$ $^{3}J_{5',4'} = 3.2$ $^{2}J_{5',5} = -12.5$

mercaptobutyl ITC is responsible for the typical sharpness and flavor. As the extracted 1,3-thiazepane-2-thione had only a light "rocket-smell", it probably contributes to a lesser extent to the rocket flavor than it's precursor ITC. It was reported that the pungent sensation of rocket immediately arises after crushing the leaves, but that it also rapidly declines and the flavor changes to green notes (Raffo et al., 2018), which could be explained by the fast cyclization of this ITC to the 1,3-thiazepane-2-thione. When we finally had the possibility to measure freshly homogenized rocket sprout tissue on a SolGel1-MS column (similar to DB-1) we observed that also a minor compound with a very similar mass spectrum to 1,3-thiazepane-2-thione [$M^{+\cdot}$ 147 (28%), 114 (100%), 87 (50%), 72 (44%), 60 (23%), 55 (29%), 47 (27%), see Supplemental Fig. 6] was present, which eluted about 2 min later and had an RI of 1486. The main difference of its mass spectrum to that of 1,3-thiazepane-2-thione (Supplemental Fig. 1) was the higher abundance of *m/z* 147. This compound so far was overlooked by us, as it was only present in low amounts in freshly homogenized tissues (and often co-eluted there with another compound) and not in the isolated 1,3-thiazepane-2-thione samples. Due to its chromatographic behavior, we suspect that this compound is the initially formed 4-mercaptobutyl ITC. In samples homogenized for 1 min at 0 °C and analyzed immediately or after 120 min, the peak area of the suspected ITC ranged between 0.09 and 0.44% of that of the 1,3-thiazepane-2-thione (and no decrease or increase was observable; data not shown), thus demonstrating the high reactivity of 4-mercaptobutyl ITC to its dithiocarbamate.

Taken together, the 1,3-thiazepane-2-thione is a very exceptional GLS hydrolysis product and its functions in plant biochemistry and human nutrition should be unraveled in the future.

4. Conclusions

The main GLS degradation product from rocket is a cyclized ITC, namely 1,3-thiazepane-2-thione. In contrast to other ITCs, this compound is quite stable, even under thermal treatment, while other ITCs from rocket are degraded. Since this compound showed no cytotoxicity on HepG2 cells at relevant concentrations for food, sativin/1,3-thiazepane-2-thione might have a less important role in GLS-related chemoprevention compared to ITC. However, the data should be validated with other cell lines and also other effects of this compound should be investigated in the future.

Acknowledgements

We thank Angela Thiesies and Marie Nickel for excellent technical assistance and Clemens Mügge for providing access to the NMR spectrometer.

Funding

Franziska S. Hanschen and this work was funded by the Deutsche Forschungsgemeinschaft (DFG) [GZ: HA 7383/2-1].

Conflict of interest

The authors declare no conflict of interest.

Appendix A. Supplementary data

Supplementary data associated with this article can be found, in the online version, at http://dx.doi.org/10.1016/j.foodchem.2018.04.023.

References

Abbehausen, C., de Paiva, R. E. F., Formiga, A. L. B., & Corbi, P. P. (2012). Studies of the tautomeric equilibrium of 1,3-thiazolidine-2-thione: theoretical and experimental approaches. *Chem. Phys. 408*, 62–68.

Agerbirk, N., & Olsen, C. E. (2012). Glucosinolate structures in evolution. *Phytochemistry, 77*, 16–45.

Agerbirk, N., & Olsen, C. E. (2015). Glucosinolate hydrolysis products in the crucifer *Barbarea vulgaris* include a thiazolidine-2-one from a specific phenolic isomer as well as oxazolidine-2-thiones. *Phytochemistry, 115*, 143–151.

Astwood, E. B., Greer, M. A., & Ettlinger, M. G. (1949). l-5-Vinyl-2-thiooxazolidone, an antithyroid compound from yellow turnip and from *Brassica* seeds. *J. Biol. Chem. 181*(1), 121–130.

Becke, A. D. (1992). Density-functional thermochemistry. I. The effect of the exchange-only gradient correction. *J. Chem. Phys. 96*(3), 2155–2160.

Becke, A. D., & Johnson, E. R. (2005). A density-functional model of the dispersion interaction. *J. Chem. Phys. 123*(15), 154101.

Bennett, R. N., Carvalho, R., Mellon, F. A., Eagles, J., & Rosa, E. A. S. (2007). Identification and quantification of glucosinolates in sprouts derived from seeds of wild *Eruca sativa* L. (salad rocket) and *Diplotaxis tenuifolia* L. (wild rocket) from diverse geographical locations. *J. Agric. Food. Chem. 55*(1), 67–74.

Bennett, R. N., Mellon, F. A., Botting, N. P., Eagles, J., Rosa, E. A. S., & Williamson, G. (2002). Identification of the major glucosinolate (4-mercaptobutyl glucosinolate) in leaves of *Eruca sativa* L. (salad rocket). *Phytochemistry, 61*(1), 25–30.

Bennett, R. N., Rosa, E. A. S., Mellon, F. A., & Kroon, P. A. (2006). Ontogenic profiling of glucosinolates, flavonoids, and other secondary metabolites in *Eruca sativa* (salad rocket), *Diplotaxis erucoides* (wall rocket), *Diplotaxis tenuifolia* (wild rocket), and *Bunias orientalis* (turkish rocket). *J. Agric. Food. Chem. 54*(11), 4005–4015.

Bruggeman, I. M., Temmink, J. H. M., & van Bladeren, P. J. (1986). Glutathione- and cysteine-mediated cytotoxicity of allyl and benzyl isothiocyanate. *Toxicol. Appl. Pharmacol. 83*(2), 349–359.

Budnowski, J., Hanschen, F. S., Lehmann, C., Haack, M., Brigelius-Flohé, R., Kroh, L. W., ... Hanske, L. (2013). A derivatization method for the simultaneous detection of glucosinolates and isothiocyanates in biological samples. *Anal. Biochem. 441*(2), 199–207.

Burow, M., & Wittstock, U. (2009). Regulation and function of specifier proteins in plants. *Phytochem. Rev. 8*(1), 87–99.

Cataldi, T. R. I., Rubino, A., Lelario, F., & Bufo, S. A. (2007). Naturally occurring

glucosinolates in plant extracts of rocket salad (*Eruca sativa* L.) identified by liquid chromatography coupled with negative ion electrospray ionization and quadrupole ion-trap mass spectrometry. *Rapid Commun. Mass Spectrom. 21*(14), 2374–2388.
Cerny, M. S., Taube, E., & Battaglia, R. (1996). Identification of bis(4-iso-thiocyanatobutyl) disulfide and its precursor from rocket salad (*Eruca sativa*). *J. Agric. Food. Chem. 44*(12), 3835–3839.
Chen, C.-W., & Ho, C.-T. (1998). Thermal degradation of allyl isothiocyanate in aqueous solution. *J. Agric. Food. Chem. 46*(1), 220–223.
Chen, C.-W., Rosen Robert, T., & Ho, C.-T. (1998). Analysis of thermal degradation products of allyl isothiocyanate and phenethyl isothiocyanate. *Flavor Analysis: vol. 705*, (pp. 152–166). American Chemical Society.
Drobnica, L., Kristián, P., & Augustín, J. (1977). The chemistry of the -NCS group. In S. Patai (Vol. Ed.), *The Chemistry of Cyanates and Their Thio Derivatives: vol. Part 2*, (pp. 1003–1221). Chichester, U.K.: Wiley.
Gaitan, E. (2004). *Goitrogens, Environmental In Encyclopedia of Endocrine Diseases.* New York: Elsevier286–294.
Halimehjani, A. Z., Marjani, K., & Ashouri, A. (2010). Synthesis of dithiocarbamate by Markovnikov addition reaction in aqueous medium. *Green Chem. 12*(7), 1306–1310.
Hanschen, F. S., Brüggemann, N., Brodehl, A., Mewis, I., Schreiner, M., Rohn, S., & Kroh, L. W. (2012). Characterization of products from the reaction of glucosinolate-derived isothiocyanates with cysteine and lysine derivatives formed in either model systems or broccoli sprouts. *J. Agric. Food. Chem. 60*(31), 7735–7745.
Hanschen, F. S., Lamy, E., Schreiner, M., & Rohn, S. (2014). Reactivity and stability of glucosinolates and their breakdown products in foods. *Angew. Chem. Int. Ed. 53*(43), 11430–11450.
Hanschen, F. S., & Schreiner, M. (2017). Isothiocyanates, nitriles, and epithionitriles from glucosinolates are affected by genotype and developmental stage in *Brassica oleracea* varieties. *Front. Plant Sci. 8*(1095).
Jin, Y., Wang, M., Rosen, R. T., & Ho, C.-T. (1999). Thermal degradation of sulforaphane in aqueous solution. *J. Agric. Food. Chem. 47*(8), 3121–3123.
Kim, S.-J., Jin, S., & Ishii, G. (2004). Isolation and structural elucidation of 4-(b-D-glucopyranosyldisulfanyl)butyl glucosinolate from leaves of rocket salad (*Eruca sativa* L.) and its antioxidative activity. *Biosci. Biotechnol. Biochem. 68*(12), 2444–2450.
Kim, S.-J., Kawaharada, C., Jin, S., Hashimoto, M., Ishii, G., & Yamauchi, H. (2007). Structural elucidation of 4-(cystein-S-yl)butyl glucosinolate from the leaves of *Eruca sativa*. *Biosci. Biotechnol. Biochem. 71*(1), 114–121.
Klamt, A., & Schuurmann, G. (1993). COSMO: a new approach to dielectric screening in solvents with explicit expressions for the screening energy and its gradient. *J. Chem. Soc., Perkin Trans. 2*(5), 799–805.
Kupke, F., Herz, C., Hanschen, F. S., Platz, S., Odongo, G. A., Helmig, S., ... Lamy, E. (2016). Cytotoxic and genotoxic potential of food-borne nitriles in a liver in vitro model. *Sci. Rep. 6*, 37631.
Lamy, E., & Mersch-Sundermann, V. (2009). MTBITC mediates cell cycle arrest and apoptosis induction in human HepG2 cells despite its rapid degradation kinetics in the in vitro model. *Environ. Mol. Mutagen. 50*(3), 190–200.
Lee, C., Yang, W., & Parr, R. G. (1988). Development of the Colle-Salvetti correlation-energy formula into a functional of the electron density. *Phys. Rev. B, 37*(2), 785–789.
Neese, F. (2012). The ORCA program system. *Wiley Interdisciplinary Reviews: Computational Molecular Science* (pp. 73–78). .
Özdemir, N., & Türkpençe, D. (2013). Theoretical investigation of thione-thiol tautomerism, intermolecular double proton transfer reaction and hydrogen bonding interactions in 4-ethyl-5-(2-hydroxyphenyl)-2H-1,2,4-triazole-3(4H)-thione. *Comput. Theor. Chem. 1025*, 35–45.
Pecháček, R., Velíšek, J., & Hrabcová, H. (1997). Decomposition products of allyl isothiocyanate in aqueous solutions. *J. Agric. Food. Chem. 45*(12), 4584–4588.
Podhradský, D., Drobnica, L., & Kristian, P. (1979). Reactions of cysteine, its derivatives, glutathione, coenzyme A, and dihydrolipoic acid with isothiocyanates. *Experientia, 35*(2), 154–155.
Radulović, N. S., Todorovska, M. M., Zlatković, D. B., Stojanović, N. M., & Randjelović, P. J. (2017). Two goitrogenic 1,3-oxazolidine-2-thione derivatives from Brassicales taxa: challenging identification, occurrence and immunomodulatory effects. *Food Chem. Toxicol. 110*, 94–108.
Raffo, A., Masci, M., Moneta, E., Nicoli, S., Sánchez del Pulgar, J., & Paoletti, F. (2018). Characterization of volatiles and identification of odor-active compounds of rocket leaves. *Food Chem. 240*, 1161–1170.
Stephens, P. J., Devlin, F. J., Chabalowski, C. F., & Frisch, M. J. (1994). Ab initio calculation of vibrational absorption and circular dichroism spectra using density functional force fields. *J. Phys. Chem. 98*(45), 11623–11627.
Veeranki, O., Bhattacharya, A., Tang, L., Marshall, J., & Zhang, Y. (2015). Cruciferous vegetables, isothiocyanates, and prevention of bladder cancer. *Curr. Pharmacol. Rep. 1*(4), 272–282.
Vosko, S. H., Wilk, L., & Nusair, M. (1980). Accurate spin-dependent electron liquid correlation energies for local spin density calculations: a critical analysis. *Can. J. Phys. 58*(8), 1200–1211.
Weigend, F. (2006). Accurate Coulomb-fitting basis sets for H to Rn. *PCCP, 8*(9), 1057–1065.
Wu, Y., Mao, J., Mei, L., & Liu, S. (2013). Kinetic studies of the thermal degradation of sulforaphane and its hydroxypropyl-beta-cyclodextrin inclusion complex. *Food Res. Int. 53*(1), 529–533.
Wu, Y., Mao, J., You, Y., & Liu, S. (2014). Study on degradation kinetics of sulforaphane in broccoli extract. *Food Chem. 155*, 235–239.
Zhang, Y., & Talalay, P. (1994). Anticarcinogenic activities of organic isothiocyanates: chemistry and mechanisms. *Cancer Res. 54*(7_Supplement), 1976–1981.